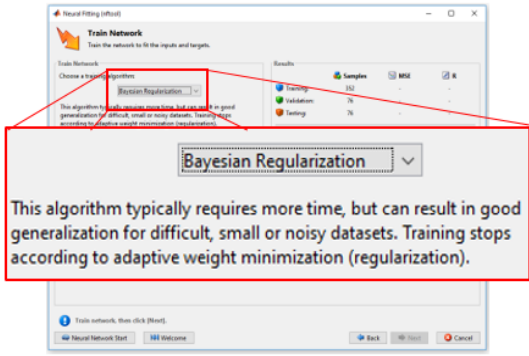
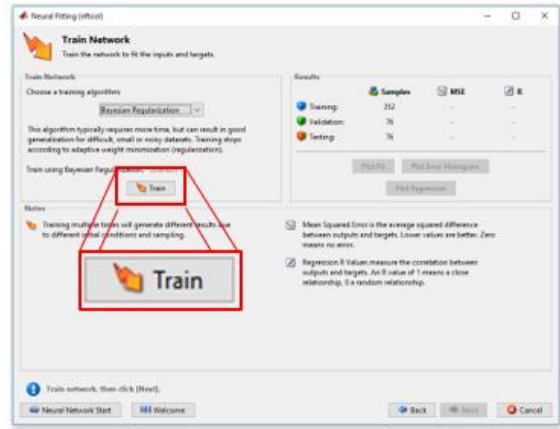
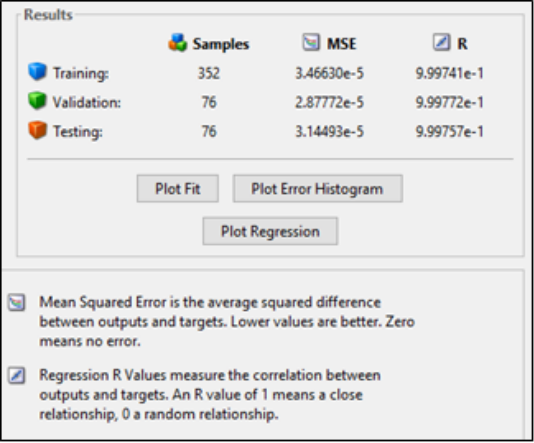


<p>3</p>	<p>The Welcome to the Neural Fitting application window was displayed and contained a block diagram of a typical Fitting ANN, a brief description of what a Fitting ANN is and examples of Fitting ANN applications. NEXT was clicked to display the Select Data window.</p>	
<p>4</p>	<p>In the Select Data window, the “Final Data” dataset was selected as the inputs and the Final Answer dataset was selected as the targets (answers).</p>	
<p>5</p>	<p>In the Validation and Test Data window, the default settings were used. NEXT was clicked to bring up the Network Architecture window.</p>	
<p>6</p>	<p>The ANN Toolbox then automatically generated an ANN from the input and output matrices provided and the result was shown in the Network Architecture window. The number of input nodes were shown as well as the number of hidden layers, output layers and outputs. The software designed the ANN to have 29 184 inputs, 10 hidden layers, 1 output layer and 1 output. NEXT was clicked to bring up the Train Network window.</p>	

<p>7</p>	<p>The Bayesian Regularization algorithm was selected as the training algorithm for the ANN.</p>																	
<p>Training step</p>																		
<p>8</p>	<p>After the preferred training algorithm was selected, training of the ANN could commence by clicking the TRAIN button in the Train Network window.</p>																	
<p>Evaluation of training step</p>																		
<p>9</p>	<p>The successful training of the ANN was evaluated by inspecting the MSE and R values in the Results window of the ANN Toolbox.</p>	 <table border="1" data-bbox="874 1211 1385 1355"> <thead> <tr> <th></th> <th>Samples</th> <th>MSE</th> <th>R</th> </tr> </thead> <tbody> <tr> <td>Training:</td> <td>352</td> <td>3.46630e-5</td> <td>9.99741e-1</td> </tr> <tr> <td>Validation:</td> <td>76</td> <td>2.87772e-5</td> <td>9.99772e-1</td> </tr> <tr> <td>Testing:</td> <td>76</td> <td>3.14493e-5</td> <td>9.99757e-1</td> </tr> </tbody> </table>		Samples	MSE	R	Training:	352	3.46630e-5	9.99741e-1	Validation:	76	2.87772e-5	9.99772e-1	Testing:	76	3.14493e-5	9.99757e-1
	Samples	MSE	R															
Training:	352	3.46630e-5	9.99741e-1															
Validation:	76	2.87772e-5	9.99772e-1															
Testing:	76	3.14493e-5	9.99757e-1															

The Results window of the software contained the results of the training procedure. The window showed the Mean Squared Error (MSE) values from 2,877e-5 to 3,466e-5, which indicated a high accuracy in training as MSE values of close to 0 were expected. The R values varied from 0,9974 to 0,9977, which further indicated a more than 99% correlation between output and target values. To

further validate the training of the ANN, linear plots for the training, validation, test as well as the overall (average) outputs were generated. The linear line in Figure 6.4 A, B, C and D indicates the targets for each output, whereas the black dots indicates the actual output for each test. The closer the proximity of each output was to the linear line, the more accurate the outputs were. From Figure 6.4 it was clear that the training of the ANN was successful as all results were in close proximity to the linear target values. After the successful training of the ANN, the ANN was exported to the Simulink environment of MATLAB to be implemented as part of the ASCS.

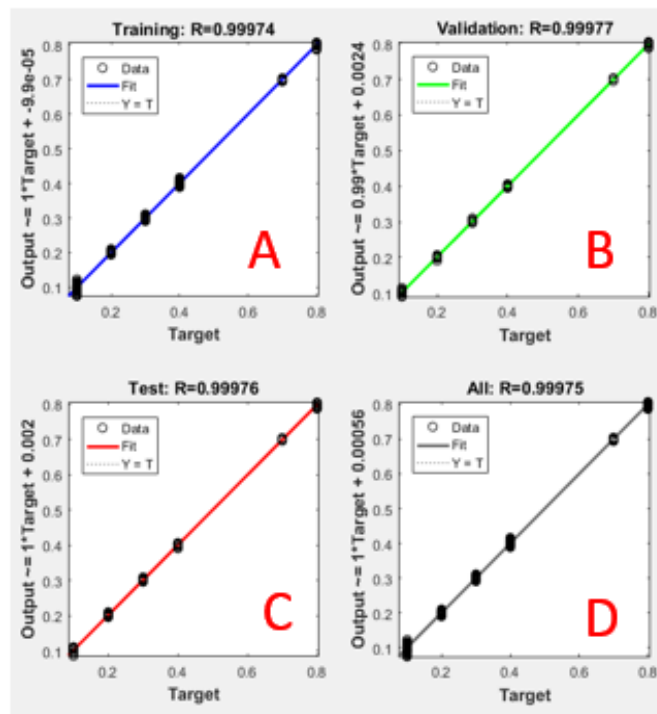


Figure 6.4 Linear plot of the ANN training results of: A) Training data, B) Validation data, C) Test data and D) Overall (average of A, B and C) data.

6.2.5 Integration of the ANN into the ASCS

To implement the ANN as part of the ASCS, the developed and trained ANN was exported to the Simulink environment of the MATLAB R2016a software. To export the ANN to the Simulink environment, the Deploy Solution window (Figure 6.5) of the ANN Toolbox software was used and the Simulink Diagram option was selected.

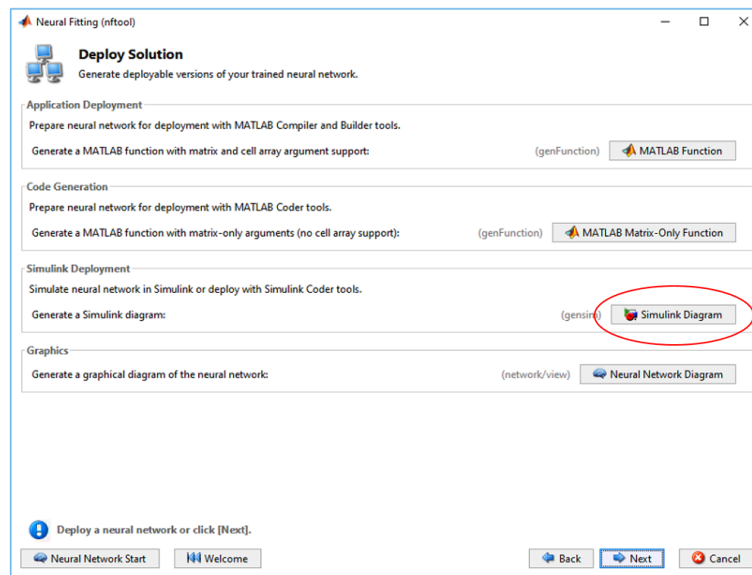


Figure 6.5 Deploy Solution window of the ANN Toolbox.

Three function blocks were automatically generated by the software and displayed in the Simulink environment. These function blocks operated together as a program to calculate results from any given input. The input for the x1 Constant block consisted of an SS fingerprint that needed to be processed by the ANN. The x1 Constant (input) block then provided the input data (SS fingerprint data) to the NNET block which represents the trained ANN. The NNET block then applied the trained ANN to the input data and the result was displayed in the y1 (output) block.

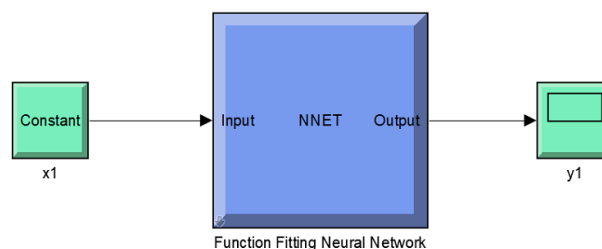


Figure 6.6 Automatically generated program displayed as a Simulink diagram.

The automatically generated Simulink program was then manually modified to improve functionality and to make the program more user-friendly. A “From Workspace” function block was added so that the SS fingerprint data (input data) that needed to be processed by the ANN could be selected directly from the MATLAB workspace environment. As the output of the NNET function block was displayed as a value between 0 and 1, a Constant function block was added to multiply the output with the Constant block value of 100, using the Product function block. The result was then shown as a percentage value in the Display function block. The modified Simulink program is shown in Figure 6.7.

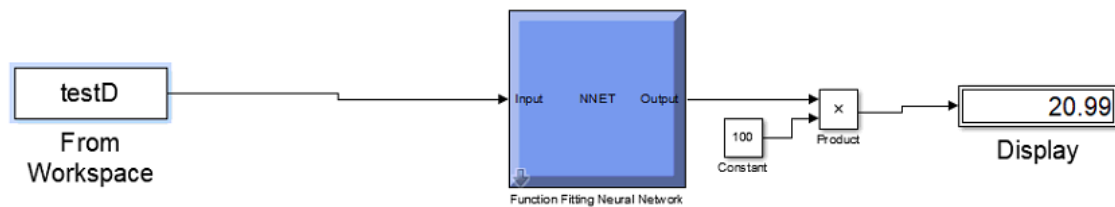


Figure 6.7 Modified Simulink program.

The user interface could be used to provide input data to the trained ANN in the form of an SS fingerprint. The SS fingerprint was then processed by the trained ANN which identified the percentage of Bentonite clay in the soil sample. Once all modifications were applied, the ANN was implemented as part of the ASCS to calculate the percentage of clay from SS fingerprints generated for soil samples by the MVI. Two investigations were undertaken to evaluate the functionality of the ANN as well as a comparison of its accuracy compared to that of the Hydrometer method.

6.3 Materials and methods for investigations 5 and 6

Two investigations were undertaken in this section. Investigation 5 was undertaken to evaluate how accurately the ASCS could determine the percentage of clay in a soil sample. Investigation 6 was undertaken to compare the results of the ASCS to that of the Hydrometer method. The details of the investigations are shown in Table 6-5.

Table 6-5 Layout of steps for Investigations 5 and 6

Investigation	Materials and methods
<p>Investigation 5: Evaluation of the accuracy of the ASCS</p>	<p>To evaluate the accuracy of the ASCS, the following steps were followed:</p> <ul style="list-style-type: none"> • Four soil samples were prepared containing 10, 20, 40 and 80% of Bentonite clay using the soil sample preparation method. • To facilitate a blind soil classification process, each soil sample was allocated a code (for example, MM04) by a third party, who kept a record of the corresponding constitutions of the soil samples. The coded soil samples were labelled as follows: <ul style="list-style-type: none"> • MM06 (Containing 10% Bentonite) • MM04 (Containing 20% Bentonite) • MM11 (Containing 40% Bentonite) • MM07 (Containing 80% Bentonite) • An SS fingerprint was generated for each coded soil samples using the MVI. • In the Simulink environment, the ANN program was provided with inputs of the SS fingerprints generated from each of the coded soil samples by the MVI. • The ANN outputs were compared to the actual amount of Bentonite clay in the coded soil samples. • The approximate amount of time it took to complete all tests were noted.
<p>Investigation 6: Comparison of both the accuracy as well as the amount of time it took for the ASCS to generate results compared to that of the Hydrometer method</p>	<p>The ASCS was compared to the Hydrometer method in the following manner:</p> <ul style="list-style-type: none"> • The same coded soil samples that were used in Investigation 5 were used to perform investigation 6 as the ASCS classification results were already known from Investigation 5. • Each coded soil sample was then also classified by means of the Hydrometer method by the soil classification laboratory of the Central University of Technology. • The output of the ASCS for each coded soil sample was then compared to the soil classification results of the Hydrometer method. • The total time it took to classify all the coded soil samples for each method was also noted for comparison.

6.4 Results of investigations

Investigation 5 were undertaken to evaluate how accurately the ASCS could determine the clay content of a soil sample. The accuracy and speed of the ASCS were then compared to that of the Hydrometer method in Investigation 6.

6.4.1 Results of Investigation 5: Evaluation of the accuracy of the ASCS

Investigation 5 was undertaken to determine how accurately the complete ASCS could determine the amount of Bentonite clay in a given soil sample. The soil classification results by the ASCS showed values with an accuracy from 95,75% to 98,50% (Table 6-6). These results showed that the ASCS was able to determine the amount of Bentonite clay in a soil sample with an accuracy of more than 95%. It took approximately 28 hours to complete all tests and included the compulsory 24 hour waiting period as specified by the Soil Sample Preparation method.

Table 6-6 Soil classification results by the ASCS.

Original sample label	New label given by third party	Actual clay content (%)	Clay content as calculated by ASCS (%)	Accuracy (%)
MM06	A	10	9,65	96,50
MM04	D	20	20,81	96,11
MM11	B	40	39,40	98,50
MM07	C	80	76,60	95,75

6.4.2 Results of Investigation 6: Comparison of the accuracy as well as the test duration of the ASCS compared to that of the Hydrometer method.

Investigation 6 was undertaken to compare the accuracy of the ASCS to that of the Hydrometer method. The duration of the classification process for each of the two procedures were also evaluated. The soil classification results by the Hydrometer method showed values with accuracy ranging between 49,26% to 88,63% (Table 6-7). These results indicated that the Hydrometer

method had a high inconsistency in its ability to classify soil samples, whereas the ASCS's accuracy was high when compared to that of the Hydrometer method. It took approximately 7 days for the soil classification laboratory at the Central University of Technology to classify all soil samples by means of the Hydrometer method. This was substantially slower than the ~28 hours taken by the ASCS.

Table 6-7 Comparison of the soil classification results by the Hydrometer method and the ASCS.

		Hydrometer method test results	ASCS test results	Hydrometer method	ASCS
Sample code	Actual % Bentonite clay	% Clay	% Bentonite clay	Accuracy (%)	Accuracy (%)
MM06	10,00	20,30	9,65	49,26	96,50
MM04	20,00	29,46	20,81	67,89	96,11
MM11	40,00	49,43	39,40	80,92	98,50
MM07	80,00	70,90	76,60	88,63	95,75
Approximate time taken to obtain results			7 days	28 hours	

6.5 Chapter discussion and summary

In Phase 5 of this study, an ANN was developed and implemented as part of the ASCS. The function of the ANN was to calculate the percentage of Bentonite clay in soil samples from the SS fingerprints that were generated for the soil samples by the MVI. Investigation 5 showed that the completed ASCS was able to determine the amount of Bentonite clay in any given soil sample with high accuracy. Phase 6 of this study compared the accuracy and duration of the soil classification processes of the ASCS and the Hydrometer method through Investigation 6. The results of Investigation 6 showed that the ASCS was more accurate and substantially quicker in classifying soil samples than the Hydrometer method.

Chapter 7

Discussion and Conclusion

7.1 Introduction

In the construction industry, one of the major considerations when designing a superstructure is which foundation should be selected for the superstructure. Foundations support superstructures by transferring the load of the structure evenly into the earth (Chang and Svenson, 2019). The selection of an appropriate foundation ensures the stability and longevity of the superstructure, whereas an inappropriate foundation type could result in damage to the superstructure, or even the collapse of such a structure (Salam and El-kady, 2017).

When selecting an appropriate foundation for a superstructure, detailed knowledge of the soil composition upon which the superstructure will be built, is critical (Bowles, 1997; Ramesh, Kuklik and Válek, 2017). In particular, the amount of clay the soil contains is a major determining factor in the selection of an appropriate foundation type (Chang and Svenson, 2019). Although there are a number of soil classification methods to determine the amount of clay in soils, a commonly used method in South Africa is the Hydrometer method that was invented by William Nicholson in 1790 (Encyclopaedia Britannica, 2013). This method is based on the sedimentation rate of the soil particles in a viscous fluid, whereby the particle size distribution is determined according to Stokes' law, which states that different sized particles will sediment at different velocities depending on their size (Das, 2018).

Two major limitations of the Hydrometer method were the inspiration to this study. Firstly, its soil classification accuracy is doubtful; and secondly, the Hydrometer method is a manual, time intensive

soil classification method (Stott and Theron, 2016). Therefore, this study was undertaken to circumvent these limitations by developing an Automated Soil Classification System (ASCS). The successfully, newly developed ASCS automatically classifies soil samples more accurately and more expeditiously by combining Machine Vision (MV) and Artificial Neural Network (ANN) technologies. In the ASCS, MV generates a digital soil sample (SS) fingerprint by taking snapshots of a soil sample's sedimentation process over time. The ANN then classifies the soil sample by identifying the digital SS fingerprint.

7.2 The Automated Soil Classification System

A primary challenge of this study was to acquire a sequence of high fidelity, greyscale images of the sedimentation process of a soil sample over time. These images were then used to create unique SS fingerprints for different compositions of soil samples. A Machine Vision Instrument (MVI) was constructed for the capturing of the high quality images in a consistent manner. The MVI acquired these images using a good quality greyscale camera in a controlled lighting environment.

A secondary challenge was to create a fingerprint-type representation of the sedimentation process that could uniquely identify soil compositions. This required a consistent soil sample preparation method, as well as a consistent SS fingerprint generation process. This was achieved by applying a soil sample preparation protocol and generating a pixel count histogram for each of the 113 snapshots taken by the MVI during the sedimentation process. These histograms were then consolidated into a single histogram by the MVI, which was referred to as the SS fingerprint. SS fingerprint consistency was evaluated by correlating several SS fingerprints; firstly, amongst SS fingerprints generated of the same soil sample; and secondly, of SS fingerprints generated from multiple soils samples with the same soil constitution prepared with the soil sample preparation protocol. Correlation amongst SS fingerprints, generated from the same soil sample, was in the order of 97%, while the correlation amongst SS fingerprints, generated from multiple soils samples

of the same constitution, was in the order of 95%. These correlations confirmed that the soil sample preparation protocol together with the MVI was able to generate SS fingerprints with high consistency.

The final challenge in this study was to automatically classify a soil sample by processing its SS fingerprint. To achieve this goal, an ANN was trained to identify soil compositions represented by their respective SS fingerprints. To accurately identify soil compositions, large volumes of data were necessary to train the ANN. To ensure the accurate classification of soil sample compositions, a large dataset was created to train the ANN. This was achieved by enlarging the original dataset of 25 SS fingerprints by adding a 3% variance to all values multiple times. This enlarged dataset that was used for training, comprised of 525 SS fingerprints, of which each SS fingerprint consisted of 29,070 values and produced training R values greater than 0,99. In the past, several attempts were made to classify soil samples using similar technologies, however because of large amounts of data that needed to be processed with limited computational power, these attempts delivered unreliable results (Tuceryan and Jain, 1998; Sudarsan *et al.*, 2018). Computational power was not a limiting factor in this study, therefore the ANN was successfully trained to classify soil samples by identifying their SS fingerprints.

Finally, the overall soil classification ability of the ASCS was compared to that of the Hydrometer method. By using blind, pre-constituted soil samples, the accuracy of the Hydrometer method proved to be relatively low, ranging from approximately 49% to 89%. In contrast, the accuracy of all the soil classifications performed by the ASCS, using the same soil samples as for the Hydrometer method, were greater than 95%. Furthermore, the ASCS produced soil classification results within 28 hours, whereas the Hydrometer method took about seven days.

7.3 Concluding remarks and future prospects

As was shown in this study, the Hydrometer Method has many challenges in terms of accuracy and speed. Experts in the field of soil classification stated that the Hydrometer method can be a lengthy process and results are sometimes inaccurate at best (Stott and Theron, 2016; Monye, 2018). Depending on the percentage of clay in a soil sample, a single soil classification by means of the Hydrometer method can take two weeks. The lengthy process combined by continuous human interaction can result in the Hydrometer method grossly underestimating the clay content of a soil sample.

By designing and developing an ASCS, the challenges posed by the Hydrometer method were circumvented. The ASCS system is shown to be more than 95% accurate in classifying soil samples and the process has been sped up from a potential two weeks to approximately twenty-eight hours. The successfully developed ASCS could be of great value to the building industry by speeding up the soil classification process immensely and ensuring the selection of appropriate foundation types for superstructures. The selection of appropriate foundation types will contribute to the stability and longevity of superstructures.

Further studies are necessary to determine how the ASCS will perform with real world soil samples as the development of the ASCS in this study was achieved by using pre-constituted soil samples.

References

Agrawal, S. *et al.* (2019) 'A novel joint histogram equalization based image contrast enhancement', *Journal of King Saud University - Computer and Information Sciences*. King Saud University.

Allievi, L. *et al.* (2018) 'On the Use of CPT for the Geotechnical Characterization of a Normally Consolidated Alluvial Clay in Hull, UK', *Cone Penetration Testing 2018 - Proceedings of the 4th International Symposium on Cone Penetration Testing, CPT 2018*, pp. 73–78.

Andersson, T., Thurley, M. J. and Carlson, J. E. (2012) 'A machine vision system for estimation of size distributions by weight of limestone particles', *Minerals Engineering*. Elsevier Ltd, 25(1), pp. 38–46.

Ashworth, J. *et al.* (2001) 'Standard procedure in the hydrometer method for particle size analysis', *Communications in Soil Science and Plant Analysis*, 32(5), pp. 633–642.

Awolusi, T. F. *et al.* (2019) 'Performance comparison of neural network training algorithms in the modeling properties of steel fiber reinforced concrete', *Heliyon*. Elsevier Ltd, 5(1), pp. 11–15.

Babcock, H. P. (2018) 'Multiplane and Spectrally-resolved Single Molecule Localization Microscopy With Industrial Grade CMOS Cameras', *Scientific Reports*. Springer US, 8(1), pp. 4–11.

Bahrami, M. *et al.* (2019) 'Develop 24 dissimilar ANNs by suitable architectures & training algorithms via sensitivity analysis to better statistical presentation: Measure MSEs between targets & ANN for Fe–CuO/Eg–Water nanofluid', *Physica A: Statistical Mechanics and its Applications*. Elsevier B.V., 519, pp. 159–168.

Bedaiwy, M. and Naguib, A. (2012) 'A Simplified Approach for Determining the Hydrometer's Dynamic Settling Depth in Particle-size Analysis', *Catena*, 97, pp. 95–103.

Bell, F. G., Cripps, J. C. and Culshaw, M. G. (1986) 'A review of the engineering behaviour of soils and rocks with respect to groundwater', *Geological Society Engineering Geology Special Publication*, 3(July 2010), pp. 1–23.

Bendix, A. (2018) *A Sinking, Leaning 58-Storey Skyscraper in San Francisco Has Now Developed a*

Crack in One Window. Available at: <https://www.businessinsider.com> (Accessed: 6 August 2018).

Bowles, J. E. (1997) *Foundation Analysis and Design*. The McGraw-Hill Companies, New York.

Chanasyk, D. S. and Naeth, M. A. (1996) 'Field measurement of soil moisture using neutron probes', *Canadian Journal of Soil Science*, 76(3), pp. 317–323.

Chang, P.-C. and Svenson, A. (2019) *Construction and Building*. Available at: <https://www.britannica.com/technology/building-construction> (Accessed: 12 September 2018).

Cowan, C. K., Modayur, B. and DeCurtins, J. L. (1992) 'Automatic light-source placement for detecting object features', *Intelligent Robots and Computer Vision XI*, 1826, pp. 12–16.

Dalsa Coreco (2017) *Choosing the Right Image Processing Software : A Machine Vision White Paper*. Available at: https://www.controldesign.com/assets/Media/MediaManager/wp_06_001_dalsa_vision.pdf (Accessed: 19 July 2018).

Das, B. M. (2011) *Principles of Foundation Engineering*. Edited by T. Altieri. Cengage Learning, Stamford.

Das, B. M. (2018) *Fundamentals of Geotechnical Engineering*. Edited by H. Gowans. Chris Carson, Madrid.

Department of Public Works, S. A. (2007) *Guideline for Problem Soils in South Africa*. Department of Public Works, South Africa.

Department of the Army (1983) 'Tm 5-818-7 Technical Manual for Foundations in Expansive Soils'. Department of the Army, U.S.A.

Dhawale, N. (2015) 'Advances in Proximal Soil Sensing Through Integrated Systems Approach'. Doctoral Thesis of the Department of Bioresource Engineering Macdonald Campus of McGill University Montreal, Canada.

Encyclopaedia Britannica (2013) *Hydrometer Measurement Instrument*. Available at:

<https://www.britannica.com/technology/hydrometer> (Accessed: 15 August 2018).

Encyclopaedia Britannica (2017) *Leaning tower of Pisa*. Available at: <https://www.britannica.com/topic/Leaning-Tower-of-Pisa> (Accessed: 20 August 2018).

Fanning, D. S. and Fanning, M. C. B. (1989) *Soil Morphology, Genesis and Classification*. John Wiley and Sons Inc.

Fell, J. (2017) *How to Choose a Machine Vision Camera*, *Quality magazine*. Available at: <https://www.qualitymag.com/> (Accessed: 16 September 2018).

Fisher, P. *et al.* (2017) 'Adequacy of Laser Diffraction for Soil Particle Size Analysis', *Plos one*. Queen's University at Kingston, Canada.

Fondjo, A. A. (2018) 'Characterization of Swelling Stress and Soil Moisture Deficiency Relationship for Expansive Unsaturated Soils'. Doctoral thesis of the School of Civil Engineering, Central University of Technology, Free State.

Frey, H. (2005) 'Machine Vision Class Notes'. Fachhochschule-Ulm, Ulm, Germany.

Ghasemy, A., Rahimi, E. and Malekzadeh, A. (2019) 'Introduction of a new method for determining the particle-size distribution of fine-grained soils', *Measurement: Journal of the International Measurement Confederation*. Elsevier Ltd, 132, pp. 79–86.

Heung, B. *et al.* (2016) 'An overview and comparison of machine-learning techniques for classification purposes in digital soil mapping', *Geoderma*. Elsevier B.V., 265, pp. 62–77.

Hillel, D. (1982) *Introduction to Soil Physics*. Academic Press Inc., Elsevier.

Jimenez-Martinez, M. and Alfaro-Ponce, M. (2019) 'Fatigue damage Effect Approach by Artificial Neural Network', *International Journal of Fatigue*, 124, pp. 42–47.

John, J. G. and N, A. (2019) 'Illumination Compensated images for surface roughness evaluation using machine vision in grinding process', *Procedia Manufacturing*. Elsevier B.V., 34, pp. 969–977.

Jones, L. D. and Jefferson, I. (2012) 'Geotechnical Engineering Principles, Problematic Soils and Site Investigation', *ICE Publishing*, 1, pp. 413–441.

Katemake, P. *et al.* (2019) 'Influence of LED-based assistive lighting solutions on the autonomous mobility of low vision people', *Building and Environment*. Elsevier, 157(December 2018), pp. 172–184.

Kaur, A. and Fanourakis, G. C. (2016) 'The effect of type, concentration and volume of dispersing agent on the magnitude of the clay content determined by the hydrometer analysis', *Journal of the South African Institution of Civil Engineering*, pp. 48–54.

Knuth, K. H. (2012) 'Optimal data-based binning for histograms and histogram-based probability density models', *Digital Signal Processing*. Elsevier Inc., 95, pp. 1–28.

Kolakshyapati, M. *et al.* (2019) 'Usefulness of histogram-profile analysis in ring-enhancing intracranial lesions', *World Neurosurgery*. Elsevier Inc, pp. 1–11.

Kopparapu, S. K. (2006) 'Lighting design for machine vision application', *Image and Vision Computing*, 24(7), pp. 720–726.

Kumar, Y., Venkatesh, K. and Kumar, V. (2012) 'Particle Size Based Assessment of Soil Using Neural Network Modeling', *Proceedings of Indian Geotechnical Conference*, (1), pp. 680–683.

Luwes, N. (2010) 'Artificial Intelligence Machine Vision Grading System'. Masters thesis of the Faculty of Engineering and Information Technology of the Central University of Technology, Free State.

Marr, B. (2017) *The Amazing Ways Google Uses Deep Learning AI*. Available at: <https://www.forbes.com/sites/bernardmarr/2017/08/08/the-amazing-ways-how-google-uses-deep-learning-ai/#1d956c9e3204> (Accessed: 1 August 2018).

Marshall, T. J. and Holmes, J. W. (1988) *Soil physics*. Cambridge University Press, Cambridge.

Merouane, F. Z. and Mamoune, S. M. A. (2018) 'Prediction of Swelling Parameters of Two Clayey Soils From Algeria Using Artificial Neural Networks', *Mathematical Modelling in Civil Engineering*,

14(3), pp. 11–26.

Minasny, B. *et al.* (2004) 'Neural Networks Prediction of Soil Hydraulic Functions for Alluvial Soils Using Multistep Outflow Data', *Soil Science Society of America Journal*, 68(2), pp. 417–429.

Mohi Alden, K. *et al.* (2019) 'Quality and shelf-life prediction of cauliflower under modified atmosphere packaging by using artificial neural networks and image processing', *Computers and Electronics in Agriculture*, 163(May).

Monye, P. K. (2018) 'Extent of Inaccuracy in The Hydrometer Test'. Masters thesis of the Faculty of Engineering and Information Technology of the Central University of Technology, Free State.

Morales, E. M. and Morales, M. K. (2004) 'Expansive Soils – Identification , Detection and Remediation Strategies', *PGA Tech*, 1, pp. 3–5.

Mukhlisin, M., Sharina, A. and Abd, B. (2017) 'Prediction of Atterberg Limits via ANN and ANFIS : a Comparison', *Journal of Geoscience, Engineering, Environment, and Technology*, 2(1), pp. 20–30.

Nakhaei, M. (2005) 'Estimating the Saturated Hydraulic Conductivity of Granular Material, Using Artificial Neural Network, Based on Grain Size Distribution Curve', *Journal of Sciences, Islamic Republic of Iran*, 16(1), pp. 55–62.

National Instruments (2009) 'Getting Started with the LabVIEW Datalogging and Supervisory Control'. National Instruments.

Nigrini, L. B. (2012) 'Developing a Neural Network Model to Predict the Electrical Load Demand in the Mangaung Municipal Area'. Doctoral thesis of the School of Electrical and Computer Systems Engineering, Central University of Technology, Free State.

Or, D. and Tuller, M. (2004) 'Soil Classification', *Chemical Engineering Science*, 1, pp. 63–69.

Parameswari, P. and Manikantan, M. (2018) 'Prediction of Soil Texture Using Feed Forward Neural Networks', *Indian J.Sci.Res*, 17(2), pp. 323–326.

Peduto, D. *et al.* (2016) 'Investigating the Behaviour of Buildings with Different Foundation Types on

Soft Soils: Two Case Studies in the Netherlands', *Procedia Engineering*, 158, pp. 529–534.

Pinnamaneni, P. (2013) 'Machine Vision Systems and Image Processing with Applications', *Journal of Innovation in Computer Science and Innovation*, 3, pp. 1–4. Available at: https://www.researchgate.net/publication/236872855_Machine_Vision_Systems_and_Image_Processing_with_Applications.

Plumb, A. P. *et al.* (2005) 'Optimisation of the predictive ability of artificial neural network (ANN) models: A comparison of three ANN programs and four classes of training algorithm', *European Journal of Pharmaceutical Sciences*, 25(4–5), pp. 395–405.

Przewlocki, J. and Zielinska, M. (2016) 'Analysis of the Behavior of Foundations of Historical Buildings', *Procedia Engineering*. The Author(s), 161, pp. 362–367.

Radcliffe, J., Cox, J. and Bulanon, D. M. (2018) 'Machine vision for orchard navigation', *Computers in Industry*. Elsevier B.V., 98, pp. 165–171.

Ramesh, M., Kuklik, P. and Válek, M. (2017) 'Several Comments on Numerical Modeling of Shallow Foundations', *Procedia Engineering*. The Author(s), 195, pp. 73–80.

Reale, C. *et al.* (2018) 'Automatic Classification of Fine-grained Soils Using CPT Measurements and Artificial Neural Networks', *Advanced Engineering Informatics*, 36, pp. 207–215.

Reingold, E. and Nightingale, J. (1999) *Artificial Neural Networks Technology*. Available at: <http://www2.psych.utoronto.ca/users/reingold/courses/ai/cache/neural3.html> (Accessed: 7 August 2019).

Rogers, J. D., Olshansky, R. and Rogers, R. B. (1993) 'Damage To Foundations From Expansive Soils', *Claims People*, 3, pp. 1–4.

Rowell, D. L. (2014) *Soil Science: Methods and Applications*. Taylor & Francis Group, London and New York.

Rukmani, P. *et al.* (2018) 'Industrial Monitoring Using Image Processing, IoT and Analyzing the Sensor Values Using Big Data', *Procedia Computer Science*. Elsevier B.V., 133, pp. 991–997.

Salam, S. A. and El-kady, M. S. (2017) 'Foundations for Low Cost Buildings', *Journal of Computational Design and Engineering*, 4, pp. 143–149.

Savage, P. F. (2007) 'Evaluation of Possible Swelling Potential of Soil', *Proceedings of the 26th South African Transport Conference*, 1, pp. 277–283.

Semeniuta, O. *et al.* (2018) 'Towards Increased Intelligence and Automatic Improvement in Industrial Vision Systems', *Procedia CIRP*. The Author(s), 67, pp. 256–261.

Shahsavari, A. *et al.* (2019) 'Experimental investigation and develop ANNs by introducing the suitable architectures and training algorithms supported by sensitivity analysis: Measure thermal conductivity and viscosity for liquid paraffin based nanofluid containing Al₂O₃ nanoparticle', *Journal of Molecular Liquids*. Elsevier B.V., 276, pp. 850–860.

Sieczka, E. . and Harding, K. G. (1992) 'Optics, Illumination, and Image Sensing for Machine Vision', 1614(March), pp. 2–10.

Stott, P. and Theron, E. (2016) 'Shortcomings in the Estimation of Clay Fraction by Hydrometer', *Journal of the South African Institution of Civil Engineering*, 58(2), pp. 14–24.

Sudarsan, B. *et al.* (2018) 'Characterizing Soil Particle Sizes Using Wavelet Analysis of Microscope Images', *Computers and Electronics in Agriculture*. Elsevier, 148(August 2017), pp. 217–225.

Sun, L. *et al.* (2019) 'Region-of-interest undersampled MRI reconstruction: A deep convolutional neural network approach', *Magnetic Resonance Imaging*. Elsevier, 63(March), pp. 185–192.

Taheri, M. H., Abbasi, M. and Khaki Jamei, M. (2019) 'Using Artificial Neural Network for Computing the Development Length of MHD Channel Flows', *Mechanics Research Communications*, 99, pp. 8–14.

Taubner, H., Roth, B. and Tippkötter, R. (2009) 'Determination of Soil Texture: Comparison of The Sedimentation Method and The Laser-Diffraction Analysis', *Journal of Plant Nutrition and Soil Science*, 172, pp. 161–171.

Tillmann, A. *et al.* (2008) 'Characterization of subsoil heterogeneity, estimation of grain size

distribution and hydraulic conductivity at the Krauthausen test site using Cone Penetration Test', *Journal of Contaminant Hydrology*, 95(1–2), pp. 57–75.

Tromp, R. B. and Watermeyer, B. E. (1992) 'A Systematic Approach to the Design and Construction of Single-Storey Residential Masonry Structures on Problem Soils', *Die Siviele Ingenieur*, pp. 83–96.

Utai, K. *et al.* (2019) 'Mass estimation of mango fruits (*Mangifera indica* L., cv. "Nam Dokmai") by linking image processing and artificial neural network', *Engineering in Agriculture, Environment and Food*. Elsevier, 12(1), pp. 103–110.

Vitton, S. J. and Sadler, L. Y. (1997) 'Particle-size analysis of soils using light scattering X-ray absorption technology', *Geotechnical Testing Journal*, 20, p. 63.

Weil, R. R. and Brady, N. C. (2016) *The Nature and Properties of Soils*. Pearson.

Williamson, M. (2019) *Machine Vision Lens Performance*, *Qualitymag*. Available at: www.qualitymag.com/V&S (Accessed: 18 July 2019).

Ye, X. W., Dong, C. Z. and Liu, T. (2016) 'A Review of Machine Vision-Based Structural Health Monitoring: Methodologies and Applications', *Journal of Sensors*, 2016, pp. 1–10.

Zhang, X. and Dahu, W. (2019) 'Application of artificial intelligence algorithms in image processing', *Journal of Visual Communication and Image Representation*. Elsevier Inc., 61, pp. 42–49.

Zhao, Z. *et al.* (2009) 'Predict soil texture distributions using an artificial neural network model', *Computers and Electronics in Agriculture*, 65(1), pp. 36–48.